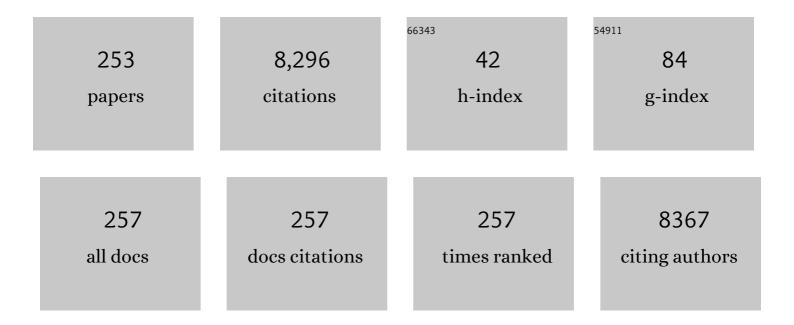
List of Publications by Year in descending order

Source: https://exaly.com/author-pdf/5344853/publications.pdf Version: 2024-02-01



#	Article	IF	CITATIONS
1	Bulk electronic structure of SrTiO3: Experiment and theory. Journal of Applied Physics, 2001, 90, 6156-6164.	2.5	782
2	Experimental and theoretical determination of the electronic structure and optical properties of three phases of ZrO2. Physical Review B, 1994, 49, 5133-5142.	3.2	476
3	Electronic Band Structure of Al2O3, with Comparison to Alon and AlN. Journal of the American Ceramic Society, 1990, 73, 477-489.	3.8	473
4	Vibrational Spectroscopy of Aluminum Nitride. Journal of the American Ceramic Society, 1993, 76, 1132-1136.	3.8	407
5	Long range interactions in nanoscale science. Reviews of Modern Physics, 2010, 82, 1887-1944.	45.6	359
6	Comparisons of Hamaker Constants for Ceramic Systems with Intervening Vacuum or Water: From Force Laws and Physical Properties. Journal of Colloid and Interface Science, 1996, 179, 460-469.	9.4	250
7	Origins and Applications of London Dispersion Forces and Hamaker Constants in Ceramics. Journal of the American Ceramic Society, 2000, 83, 2117-2146.	3.8	227
8	Optical Properties of Aluminum Oxide: Determined from Vacuum Ultraviolet and Electron Energy‣oss Spectroscopies. Journal of the American Ceramic Society, 1998, 81, 2549-2557.	3.8	174
9	Parametric tip model and force–distance relation for Hamaker constant determination from atomic force microscopy. Journal of Applied Physics, 1996, 80, 6081-6090.	2.5	173
10	Temperature dependence of the electronic structure of oxides: MgO, MgAl2O4and Al2O3. Physica Scripta, 1990, 41, 537-541.	2.5	139
11	Thin Glass Film between Ultrafine Conductor Particles in Thick-Film Resistors. Journal of the American Ceramic Society, 1994, 77, 1143-1152.	3.8	136
12	Optical properties of Teflon [®] AF amorphous fluoropolymers. Journal of Micro/ Nanolithography, MEMS, and MOEMS, 2008, 7, 033010.	0.9	126
13	Electronic structure of β-BaB2O4andLiB3O5nonlinear optical crystals. Physical Review B, 1991, 44, 8496-8502.	3.2	124
14	Heteroepitaxy of N-type β-Ga2O3 thin films on sapphire substrate by low pressure chemical vapor deposition. Applied Physics Letters, 2016, 109, .	3.3	122
15	Full spectral calculation of non-retarded Hamaker constants for ceramic systems from interband transition strengths. Solid State Ionics, 1995, 75, 13-33.	2.7	105
16	Optical reflectivity measurements using a laser plasma light source. Applied Physics Letters, 1989, 55, 1955-1957.	3.3	102
17	Multiple scattering from rutile TiO2 particles. Acta Materialia, 2000, 48, 4571-4576.	7.9	93
18	Optical properties and London dispersion interaction of amorphous and crystallineSiO2determined by vacuum ultraviolet spectroscopy and spectroscopic ellipsometry. Physical Review B, 2005, 72, .	3.2	90

#	Article	IF	CITATIONS
19	Electronic structure of aluminum nitride: Theory and experiment. Applied Physics Letters, 1993, 63, 1182-1184.	3.3	81
20	Immersion Lithography: Photomask and Wafer-Level Materials. Annual Review of Materials Research, 2009, 39, 93-126.	9.3	81
21	Optical properties of polymeric materials for concentrator photovoltaic systems. Solar Energy Materials and Solar Cells, 2011, 95, 2077-2086.	6.2	74
22	Roomâ€ŧemperature optical absorption in undoped αâ€Al2O3. Journal of Applied Physics, 1990, 67, 7542-7546.	2.5	73
23	Lightâ€Scattering Properties of Representative, Morphological Rutile Titania Particles Studied Using a Finiteâ€Element Method. Journal of the American Ceramic Society, 1998, 81, 469-479.	3.8	68
24	Interband Electronic Structure of alpha-Alumina up to 2167 K. Journal of the American Ceramic Society, 1994, 77, 412-422.	3.8	66
25	Critical point analysis of the interband transition strength of electrons. Journal Physics D: Applied Physics, 1996, 29, 1740-1750.	2.8	66
26	Optical properties of AlN determined by vacuum ultraviolet spectroscopy and spectroscopic ellipsometry data. Journal of Materials Research, 1999, 14, 4337-4344.	2.6	65
27	Lithographically Cut Single-Walled Carbon Nanotubes:  Controlling Length Distribution and Introducing End-Group Functionality. Nano Letters, 2003, 3, 1007-1012.	9.1	63
28	Automated Pipeline for Photovoltaic Module Electroluminescence Image Processing and Degradation Feature Classification. IEEE Journal of Photovoltaics, 2019, 9, 1324-1335.	2.5	63
29	Selfconsistent band structures and optical calculations in cubic ferroelectric perovskites. Ferroelectrics, 1990, 111, 23-32.	0.6	61
30	Valence electron energy loss study of Fe-doped SrTiO3 and a Σ13 boundary: electronic structure and dispersion forces. Ultramicroscopy, 2001, 86, 303-318.	1.9	61
31	Optical Properties and London Dispersion Forces of Amorphous Silica Determined by Vacuum Ultraviolet Spectroscopy and Spectroscopic Ellipsometry. Journal of the American Ceramic Society, 2003, 86, 1885-1892.	3.8	60
32	Quantitative analysis of valence electron energyâ€loss spectra of aluminium nitride. Journal of Microscopy, 1998, 191, 286-296.	1.8	59
33	van der Waals–London dispersion interactions for optically anisotropic cylinders: Metallic and semiconducting single-wall carbon nanotubes. Physical Review B, 2007, 76, .	3.2	59
34	Cu deposition on Al2O3and AlN surfaces: Electronic structure and bonding. Journal of Applied Physics, 1987, 62, 2286-2289.	2.5	54
35	Novel hydrofluorocarbon polymers for use as pellicles in 157 nm semiconductor photolithography: fundamentals of transparency. Journal of Fluorine Chemistry, 2003, 122, 63-80.	1.7	53
36	Fluid refractive index measurements using rough surface and prism minimum deviation techniques. Journal of Vacuum Science & Technology an Official Journal of the American Vacuum Society B, Microelectronics Processing and Phenomena, 2004, 22, 3450.	1.6	53

#	Article	IF	CITATIONS
37	Design rules for nanomedical engineering: from physical virology to the applications of virus-based materials in medicine. Journal of Biological Physics, 2013, 39, 301-325.	1.5	53
38	Quantitative, FFT-Based, Kramers-Krönig Analysis for Reflectance Data. Applied Spectroscopy, 1989, 43, 1498-1501.	2.2	52
39	Nonadditivity in van der Waals interactions within multilayers. Journal of Chemical Physics, 2006, 124, 044709.	3.0	51
40	Degradation science: Mesoscopic evolution and temporal analytics of photovoltaic energy materials. Current Opinion in Solid State and Materials Science, 2015, 19, 212-226.	11.5	51
41	Optical Properties and van der Waals - London Dispersion Interactions of Polystyrene Determined by Vacuum Ultraviolet Spectroscopy and Spectroscopic Ellipsometry. Australian Journal of Chemistry, 2007, 60, 251.	0.9	50
42	Statistical and Domain Analytics Applied to PV Module Lifetime and Degradation Science. IEEE Access, 2013, 1, 384-403.	4.2	50
43	Optical analysis of complex multilayer structures using multiple data types. , 1994, 2253, 1098.		43
44	Kramers–Kronig transform for the surface energy loss function. Journal of Electron Spectroscopy and Related Phenomena, 2005, 142, 97-103.	1.7	43
45	Differential degradation patterns of photovoltaic backsheets at the array level. Solar Energy, 2018, 163, 62-69.	6.1	42
46	Disentangling the Effects of Shape and Dielectric Response in van der Waals Interactions between Anisotropic Bodies. Journal of Physical Chemistry C, 2015, 119, 19083-19094.	3.1	41
47	Implication of the solvent effect, metal ions and topology in the electronic structure and hydrogen bonding of human telomeric G-quadruplex DNA. Physical Chemistry Chemical Physics, 2016, 18, 21573-21585.	2.8	41
48	Data-Driven \$I\$–\$V\$ Feature Extraction for Photovoltaic Modules. IEEE Journal of Photovoltaics, 2019, 9, 1405-1412.	2.5	41
49	Impact of environmental variables on the degradation of photovoltaic components and perspectives for the reliability assessment methodology. Solar Energy, 2020, 199, 425-436.	6.1	41
50	A Nonrelational Data Warehouse for the Analysis of Field and Laboratory Data From Multiple Heterogeneous Photovoltaic Test Sites. IEEE Journal of Photovoltaics, 2017, 7, 230-236.	2.5	40
51	Interband electronic structure of a near- grain boundary in -alumina determined by spatially resolved valence electron energy-loss spectroscopy. Journal Physics D: Applied Physics, 1996, 29, 1751-1760.	2.8	39
52	Calculating van der Waals-London dispersion spectra and Hamaker coefficients of carbon nanotubes in water from ab initio optical properties. Journal of Applied Physics, 2007, 101, 054303.	2.5	39
53	Electronic structure and interatomic bonding of crystalline β-BaB2O4with comparison toLiB3O5. Physical Review B, 1993, 48, 17695-17702.	3.2	38
54	Design of very transparent fluoropolymer resists for semiconductor manufacture at 157 nm. Journal of Fluorine Chemistry, 2003, 122, 11-16.	1.7	38

#	Article	IF	CITATIONS
55	Design and Construction of a â^1⁄47× Low-Concentration Photovoltaic System Based on Compound Parabolic Concentrators. IEEE Journal of Photovoltaics, 2012, 2, 382-386.	2.5	36
56	Chirality-dependent properties of carbon nanotubes: electronic structure, optical dispersion properties, Hamaker coefficients and van der Waals–London dispersion interactions. RSC Advances, 2013, 3, 823-842.	3.6	36
57	Laser-plasma sourced, temperature dependent, VUV spectrophotometer using dispersive analysis. Physica Scripta, 1990, 41, 404-408.	2.5	35
58	Local Optical Properties, Electron Densities, and London Dispersion Energies of Atomically Structured Grain Boundaries. Physical Review Letters, 2004, 93, 227201.	7.8	35
59	Generalized and Mechanistic PV Module Performance Prediction From Computer Vision and Machine Learning on Electroluminescence Images. IEEE Journal of Photovoltaics, 2020, 10, 878-887.	2.5	35
60	Electronic Structure, Dielectric Response and Surface Charge Distribution of RGD (1FUV) Peptide. Scientific Reports, 2014, 4, 5605.	3.3	33
61	Drivers for the cracking of multilayer polyamideâ€based backsheets in field photovoltaic modules: Inâ€depth degradation mapping analysis. Progress in Photovoltaics: Research and Applications, 2020, 28, 704-716.	8.1	33
62	Determination of the second virial coefficient of bovine serum albumin under varying pH and ionic strength by composition-gradient multi-angle static light scattering. Journal of Biological Physics, 2015, 41, 85-97.	1.5	32
63	Photodegradation in a stress and response framework: poly(methyl methacrylate) for solar mirrors and lens. Journal of Photonics for Energy, 2012, 2, 022004.	1.3	31
64	Optical superlattices—a strategy for designing phase-shift masks for photolithography at 248 and 193 nm: Application to AlN/CrN. Applied Physics Letters, 1997, 70, 2371-2373.	3.3	29
65	Computation of Light Scattering by Anisotropic Spheres of Rutile Titania. Advanced Materials, 1998, 10, 1271-1276.	21.0	29
66	Theoretical and experimental studies on Cu metallization of Al2O3. Physica B: Physics of Condensed Matter & C: Atomic, Molecular and Plasma Physics, Optics, 1988, 150, 44-46.	0.9	28
67	Optical absorption in undoped yttrium aluminum garnet. Journal of Applied Physics, 1990, 68, 1200-1204.	2.5	28
68	Electronic Structure of a Near Σ11 aâ€axis Tilt Grain Boundary in αâ€A12O3. Journal of the American Ceramic Society, 1996, 79, 627-633.	3.8	28
69	Mapping Multivariate Influence of Alloying Elements on Creep Behavior for Design of New Martensitic Steels. Metallurgical and Materials Transactions A: Physical Metallurgy and Materials Science, 2019, 50, 3106-3120.	2.2	28
70	Optical properties of materials for concentrator photovoltaic systems. , 2009, , .		27
71	Electronic Structure and Partial Charge Distribution of Doxorubicin in Different Molecular Environments. ChemPhysChem, 2015, 16, 1451-1460.	2.1	26
72	Predictive models of poly(ethylene-terephthalate) film degradation under multi-factor accelerated weathering exposures. PLoS ONE, 2017, 12, e0177614.	2.5	26

#	Article	IF	CITATIONS
73	New Amorphous Fluoropolymers of Tetrafluoroethylene with Fluorinated and Non-Fluorinated Tricyclononenes. Semiconductor Photoresists for Imaging at 157 and 193 nm. Macromolecules, 2006, 39, 3252-3261.	4.8	25
74	International collaboration framework for the calculation of performance loss rates: Data quality, benchmarks, and trends (towards a uniform methodology). Progress in Photovoltaics: Research and Applications, 2021, 29, 573-602.	8.1	25
75	Insights into metastability of photovoltaic materials at the mesoscale through massive <i>l–V</i> analytics. Journal of Vacuum Science and Technology B:Nanotechnology and Microelectronics, 2016, 34, .	1.2	24
76	Second generation fluids for 193 nm immersion lithography. , 2005, 5754, 427.		23
77	First-principles investigation of the optical properties of crystalline poly(di-n-hexylsilane). Physical Review B, 1996, 54, 13546-13550.	3.2	22
78	Building electricity consumption: Data analytics of building operations with classical time series decomposition and case based subsetting. Energy and Buildings, 2018, 177, 184-196.	6.7	22
79	New materials for 157-nm photoresists: characterization and properties. , 2000, , .		21
80	Light scattering from red pigment particles: Multiple scattering in a strongly absorbing system. Journal of Applied Physics, 2001, 89, 283-293.	2.5	21
81	Data-driven evaluation of HVAC operation and savings in commercial buildings. Applied Energy, 2020, 278, 115505.	10.1	21
82	Optical and electrical properties of niobium carbide. Physical Review B, 1987, 35, 2573-2582.	3.2	20
83	Optical properties of a near- axis tilt grain boundary in. Journal Physics D: Applied Physics, 1996, 29, 1761-1766. Imaging of 32-nm <inline-formula><math <="" altimg="none" display="inline" td=""><td>2.8</td><td>20</td></math></inline-formula>	2.8	20
84	overflow="scroll"> <mrow><mn>1</mn><mo>:</mo><mn>1</mn></mrow> lines and spaces using 193-nm immersion interference lithography with second-generation immersion fluids to achieve a numerical aperture of 1.5 and a <inline-formula><math <br="" display="inline">altimg="none" overflow="scroll"><mrow><msub><mi< td=""><td>0.9</td><td>20</td></mi<></msub></mrow></math></inline-formula>	0.9	20
85	mathvariant="normal">k <mn>1 of 0.25. Journal Graded interface models for more accurate determination of van der Waals–London dispersion interactions across grain boundaries. Physical Review B, 2006, 74, .</mn>	3.2	20
86	Dataâ€driven glass/ceramic science research: Insights from the glass and ceramic and data science/informatics communities. Journal of the American Ceramic Society, 2019, 102, 6385-6406.	3.8	20
87	Bis(fluoroalcohol) Monomers and Polymers:Â Improved Transparency Fluoropolymer Photoresists for Semiconductor Photolithography at 157 nm. Macromolecules, 2006, 39, 1443-1448.	4.8	19
88	Degradation of transparent conductive oxides: Interfacial engineering and mechanistic insights. Solar Energy Materials and Solar Cells, 2015, 143, 529-538.	6.2	19
89	Optical analysis of complex multilayer structures using multiple data types. Thin Solid Films, 1994, 253, 25-27.	1.8	18

90 Immersion fluid refractive indices using prism minimum deviation techniques. , 2004, 5377, 1689.

#	Article	IF	CITATIONS
91	Second generation fluids for 193nm immersion lithography. , 2006, , .		18
92	Solar radiation durability of materials components and systems for Low Concentration Photovoltaic Systems. , 2011, , .		18
93	Degradation in PV encapsulation transmittance: An interlaboratory study towards a climate-specific test. , 2015, , .		18
94	Charge distribution and hydrogen bonding of a collagen α ₂ â€chain in vacuum, hydrated, neutral, and charged structural models. International Journal of Quantum Chemistry, 2016, 116, 681-691.	2.0	18
95	Band Structure Calculations of the High-Temperature Electronic Structure of Magnesium Oxide. Journal of the American Ceramic Society, 1990, 73, 3195-3199.	3.8	17
96	Attenuated phase-shifting photomasks fabricated from Cr-based embedded shifter blanks. , 1994, 2254, 64.		17
97	High-index immersion lithography with second-generation immersion fluids to enable numerical aperatures of 1.55 for cost effective 32-nm half pitches. , 2007, 6520, 639.		17
98	Optical properties and electronic transitions of DNA oligonucleotides as a function of composition and stacking sequence. Physical Chemistry Chemical Physics, 2015, 17, 4589-4599.	2.8	17
99	van der Waals Interactions on the Mesoscale: Open-Science Implementation, Anisotropy, Retardation, and Solvent Effects. Langmuir, 2015, 31, 10145-10153.	3.5	17
100	Temporal evolution and pathway models of poly(ethylene-terephthalate) degradation under multi-factor accelerated weathering exposures. PLoS ONE, 2019, 14, e0212258.	2.5	17
101	Fluoropolymers for 157-nm lithography: optical properties from VUV absorbance and ellipsometry measurements. , 2000, 4000, 1491.		16
102	Reflection electron energy loss spectroscopy of nanometric oxide layers and of their interfaces with a substrate. Materials Science & Engineering A: Structural Materials: Properties, Microstructure and Processing, 2006, 422, 29-40.	5.6	16
103	Adhesive interactions of geckos with wet and dry fluoropolymer substrates. Journal of the Royal Society Interface, 2015, 12, 20150464.	3.4	16
104	Multivariate multiple regression models of poly(ethylene-terephthalate) film degradation under outdoor and multi-stressor accelerated weathering exposures. PLoS ONE, 2018, 13, e0209016.	2.5	16
105	Vacuum ultraviolet spectroscopy of the optical properties and electronic structure of seven poly(di-alkylsilanes). Synthetic Metals, 1992, 50, 499-508.	3.9	15
106	Insights into the Electronic Structure of Ceramics through Quantitative Analysis of Valence Electron Energy-loss Spectroscopy. Microscopy and Microanalysis, 2000, 6, 297-306.	0.4	15
107	Materials design and development of fluoropolymers for use as pellicles in 157-nm photolithography. , 2001, , .		15
108	Degradation of poly(ethylene-terephthalate) under accelerated weathering exposures. , 2015, , .		15

#	Article	IF	CITATIONS
109	Feature Extraction, Supervised and Unsupervised Machine Learning Classification of PV Cell Electroluminescence Images. , 2018, , .		15
110	Performance Loss Rate Consistency and Uncertainty Across Multiple Methods and Filtering Criteria. , 2019, , .		15
111	Electrical breakdown of insulating ceramics in a high-radiation field. Journal of Nuclear Materials, 1994, 217, 32-47.	2.7	14
112	<title>Materials screening for attenuating embedded phase-shift photoblanks for DUV and 193-nm photolithography</title> . , 1996, , .		14
113	157-nm imaging using thick single-layer resists. , 2001, , .		14
114	Soiling of building envelope surfaces and its effect on solar reflectance – Part III: Interlaboratory study of an accelerated aging method for roofing materials. Solar Energy Materials and Solar Cells, 2015, 143, 581-590.	6.2	14
115	Fluorescence imaging analysis of depthâ€dependent degradation in photovoltaic laminates: insights to the failure. Progress in Photovoltaics: Research and Applications, 2020, 28, 122-134.	8.1	14
116	Motivation, benefits, and challenges for new photovoltaic material & module developments. Progress in Energy, 2022, 4, 032003.	10.9	14
117	Effect of Residual Strain on the Electronic Structure of Alumina and Magnesia. Journal of the American Ceramic Society, 1989, 72, 990-994.	3.8	13
118	Simulated measurement of small metal clusters by frequency-modulation non-contact atomic force microscopy. Nanotechnology, 2006, 17, S121-S127.	2.6	13
119	Solar radiation durability framework applied to acrylic solar mirrors. , 2011, , .		13
120	Democratizing an electroluminescence imaging apparatus and analytics project for widespread data acquisition in photovoltaic materials. Review of Scientific Instruments, 2016, 87, 085109.	1.3	13
121	Electroluminescent Image Processing and Cell Degradation Type Classification via Computer Vision and Statistical Learning Methodologies. , 2017, , .		13
122	<i>Analytic</i> \$I_{ext{sc}}\$–\$V_{ext{oc}}\$ Method and Power Loss Modes From Outdoor Time-Series \$I\$–\$V\$ Curves. IEEE Journal of Photovoltaics, 2020, 10, 1379-1388.	2.5	13
123	Characterizing photovoltaic backsheet adhesion degradation using the wedge and single cantilever beam tests, Part II: Accelerated tests. Solar Energy Materials and Solar Cells, 2020, 211, 110524.	6.2	13
124	Automated pipeline framework for processing of large-scale building energy time series data. PLoS ONE, 2020, 15, e0240461.	2.5	13
125	157 nm Pellicles (Thin Films) for Photolithography:Â Mechanistic Investigation of the VUV and UV-C Photolysis of Fluorocarbons. Journal of the American Chemical Society, 2005, 127, 8320-8327.	13.7	12
126	Spectral mixing formulations for van der Waals–London dispersion interactions between multicomponent carbon nanotubes. Journal of Applied Physics, 2008, 104, 53513.	2.5	12

#	Article	IF	CITATIONS
127	Degradation in PV encapsulant strength of attachment: An interlaboratory study towards a climate-specific test. , 2016, , .		12
128	Organofunctional Silane Modification of Aluminum-Doped Zinc Oxide Surfaces as a Route to Stabilization. ACS Applied Materials & amp; Interfaces, 2017, 9, 17620-17628.	8.0	12
129	Screening of heritage data for improving toughness of creep-resistant martensitic steels. Materials Science & Engineering A: Structural Materials: Properties, Microstructure and Processing, 2019, 763, 138142.	5.6	12
130	Fluoropolymers for 157 nm Lithography: Performance of Single Layer Resists Journal of Photopolymer Science and Technology = [Fotoporima Konwakai Shi], 2002, 15, 677-687.	0.3	11
131	Behavior of candidate organic pellicle materials under 157-nm laser irradiation. , 2002, 4691, 1644.		11
132	157-nm pellicles: polymer design for transparency and lifetime. , 2002, 4691, 576.		11
133	Fluid-photoresist interactions and imaging in high-index immersion lithography. Journal of Micro/ Nanolithography, MEMS, and MOEMS, 2009, 8, 033006.	0.9	11
134	Van der Waals-London dispersion interaction framework for experimentally realistic carbon nanotube systems. International Journal of Materials Research, 2010, 101, 27-42.	0.3	10
135	Microinverter Thermal Performance in the Real-World: Measurements and Modeling. PLoS ONE, 2015, 10, e0131279.	2.5	10
136	Multiscale Characterization of Photovoltaic Modules—Case Studies of Contact and Interconnect Degradation. IEEE Journal of Photovoltaics, 2022, 12, 62-72.	2.5	10
137	Transparent fluids for 157-nm immersion lithography. Journal of Micro/ Nanolithography, MEMS, and MOEMS, 2004, 3, 73.	0.9	9
138	Synthesis, structural analysis, and self-assembly of phenylene ethynylene oligomers and their F, CF3, and CH3substituted derivatives. Journal of Polymer Science Part A, 2004, 42, 541-550.	2.3	9
139	Evaluation of Next Generation Fluids for ArF Immersion Lithography Beyond Water. Journal of Photopolymer Science and Technology = [Fotoporima Konwakai Shi], 2007, 20, 729-738.	0.3	9
140	Global SunFarm data acquisition network, energy CRADLE, and time series analysis. , 2013, , .		9
141	Dielectric response variation and the strength of van der Waals interactions. Journal of Colloid and Interface Science, 2014, 417, 278-284.	9.4	9
142	Materials data analytics for 9% Cr family steel. Statistical Analysis and Data Mining, 2019, 12, 290-301.	2.8	9
143	Characterizing photovoltaic backsheet adhesion degradation using the wedge and single cantilever beam tests, Part I: Field Modules. Solar Energy Materials and Solar Cells, 2020, 215, 110669.	6.2	9
144	Materials for Concentrator Photovoltaic Systems: Optical Properties and Solar Radiation Durability. AIP Conference Proceedings, 2010, , .	0.4	8

#	Article	IF	CITATIONS
145	Optically anisotropic infinite cylinder above an optically anisotropic half space: Dispersion interaction of a single-walled carbon nanotube with a substrate. Journal of Vacuum Science and Technology B:Nanotechnology and Microelectronics, 2010, 28, C4A17-C4A24.	1.2	8
146	Durability of acrylic: Stress and response characterization of materials for photovoltaics. , 2012, , .		8
147	Evaluation of Photovoltaic Module Performance Using Novel Data-driven I-V Feature Extraction and Suns-V _{OC} Determined from Outdoor Time-Series I-V Curves. , 2018, , .		8
148	Employing Weibull Analysis and Weakest Link Theory to Resolve Crystalline Silicon PV Cell Strength Between Bare Cells and Reduced- and Full-Sized Modules. IEEE Journal of Photovoltaics, 2021, 11, 731-741.	2.5	8
149	Vacuum-ultraviolet spectroscopy of dialkyl polysilanes. Physical Review B, 1991, 43, 10008-10011.	3.2	7
150	Consequence of Nanometerâ€Scale Property Variations to Macroscopic Properties of CrOCN Thin Films. Journal of the American Ceramic Society, 2001, 84, 2873-2881.	3.8	7
151	Single layer fluropolymer resists for 157-nm lithography. , 2003, , .		7
152	Index of refraction of high-index lithographic immersion fluids and its variability. Journal of Micro/ Nanolithography, MEMS, and MOEMS, 2009, 8, 023005.	0.9	7
153	Degradation of back surface acrylic mirrors: Implications for low concentration and mirror augmented photovoltaics. , 2012, , .		7
154	Design Considerations and Measured Performance of Nontracked Mirror-Augmented Photovoltaics. IEEE Journal of Photovoltaics, 2015, 5, 917-925.	2.5	7
155	Generalized Spatio-Temporal Model of Backsheet Degradation From Field Surveys of Photovoltaic Modules. IEEE Journal of Photovoltaics, 2019, 9, 1374-1381.	2.5	7
156	Purity of Aluminum Hydroxide Derived from Triethylaluminum. Journal of the American Ceramic Society, 1988, 71, C-204-C-206.	3.8	6
157	Near-field scattering from red pigment particles: Absorption and spectral dependence. Journal of Applied Physics, 2001, 89, 1898.	2.5	6
158	Durability of Materials in a Stress-Response Framework: Acrylic Materials for Photovoltaic Systems. Materials Research Society Symposia Proceedings, 2012, 1391, 107.	0.1	6
159	Degradation pathway models for photovoltaics module lifetime performance. , 2013, , .		6
160	Optical Properties and van der Waals–London Dispersion Interactions in Berlinite Aluminum Phosphate from Vacuum Ultraviolet Spectroscopy. Journal of the American Ceramic Society, 2014, 97, 1143-1150.	3.8	6
161	X-ray characterization of mesophases of human telomeric G-quadruplexes and other DNA analogues. Scientific Reports, 2016, 6, 27079.	3.3	6
162	Determining the Power Rate of Change of 353 Plant Inverters Time-Series Data Across Multiple Climate Zones, Using a Month-By-Month Data Science Analysis. , 2017, , .		6

#	Article	IF	CITATIONS
163	Degradation Processes and Mechanisms of Backsheets. , 2019, , 153-174.		6
164	A cross-sectional study of the temporal evolution of electricity consumption of six commercial buildings. PLoS ONE, 2017, 12, e0187129.	2.5	6
165	Detection of Optically Excited States in Wide-Band-Gap Semiconductors with Tunneling Spectroscopy. Journal of the American Ceramic Society, 1990, 73, 3257-3263.	3.8	5
166	<title>Chromium-based attenuated embedded shifter preproduction</title> . , 1994, , .		5
167	157-nm pellicles for photolithography: mechanistic investigation of the deep-UV photolysis of fluorocarbons. , 2004, 5377, 1598.		5
168	New perspectives on van der Waals–London interactions of materials. From planar interfaces to carbon nanotubes. Journal of Physics: Conference Series, 2008, 94, 012001.	0.4	5
169	Mirror-augmented photovoltaic designs and performance. , 2012, , .		5
170	Surface Antireflection and Light Extraction Properties of GaN Microdomes. IEEE Photonics Journal, 2015, 7, 1-9.	2.0	5
171	Physics-Informed Network Models: a Data Science Approach to Metal Design. Integrating Materials and Manufacturing Innovation, 2017, 6, 279-287.	2.6	5
172	Reciprocity and spectral effects of the degradation of poly(ethyleneâ€ŧerephthalate) under accelerated weathering exposures. Journal of Applied Polymer Science, 2019, 136, 47589.	2.6	5
173	Real-world PV Module Degradation across Climate Zones Determined from Suns-V _{oc} , Loss Factors and I-V Steps Analysis of Eight Years of I-V, P _{mp} Time-series Datastreams. , 2019, , .		5
174	Data analytics applied to the electricity consumption of office buildings to reveal building operational characteristics. Advances in Building Energy Research, 2020, , 1-19.	2.3	5
175	Degradation Pathway Modeling of PV Minimodule Variants with Different Packaging Materials Under Indoor Accelerated Exposures. , 2021, , .		5
176	Identifying Degradation Modes of Photovoltaic Modules Using Unsupervised Machine Learning on Electroluminescense Images. , 2020, , .		5
177	Robert L. Coble: A Retrospective. Journal of the American Ceramic Society, 1994, 77, 293-297.	3.8	4
178	Optical properties, electronic structure and London dispersion interactions for nanostructured interfacial and surficial films. Materials Science & Engineering A: Structural Materials: Properties, Microstructure and Processing, 2006, 422, 136-146.	5.6	4
179	High Refractive Index Fluid Evaluations at 193nm: Fluid Lifetime and Fluid/Resist Interaction Studies. Journal of Photopolymer Science and Technology = [Fotoporima Konwakai Shi], 2008, 21, 631-639.	0.3	4
180	High-index immersion fluids enabling cost-effective single-exposure lithography for 32 nm half pitches. , 2008, , .		4

#	Article	IF	CITATIONS
181	Degradation of transparent conductive oxides: mechanistic insights across configurations and exposures. , 2013, , .		4
182	Degradation of Transparent Conductive Oxides, and the Beneficial Role of Interfacial Layers. Materials Research Society Symposia Proceedings, 2013, 1537, 1.	0.1	4
183	Photovoltaic lifetime and degradation science statistical pathway development: acrylic degradation. Proceedings of SPIE, 2013, , .	0.8	4
184	Optical properties of PV backsheets: key indicators of module performance and durability. , 2014, , .		4
185	Correlation of I-V Curve Parameters with Module-Level Electroluminescent Image Data Over 3000 Hours Damp-Heat Exposure. , 2017, , .		4
186	Degradation Science and Pathways in PV Systems. , 2019, , 47-93.		4
187	Direct nanoscale mapping of open circuit voltages at local back surface fields for PERC solar cells. Journal of Materials Science, 2020, 55, 11501-11511.	3.7	4
188	Measurement of crack length in width tapered beam experiments. Journal of Adhesion Science and Technology, 2021, 35, 357-374.	2.6	4
189	Optical superlattices as phase-shift masks for microlithography. , 1999, , .		3
190	Insights into the Electronic Structure of Ceramics through Quantitative Analysis of Valence Electron Energy-loss Spectroscopy. Microscopy and Microanalysis, 2000, 6, 297-306.	0.4	3
191	Design and performance of a low-cost acrylic reflector for a ~7x concentrating photovoltaic module. , 2011, , .		3
192	Degradation of back surface acrylic mirrors for low concentration and mirror-augmented photovoltaics. Proceedings of SPIE, 2012, , .	0.8	3
193	Statistical and domain analytics for informed study protocols. , 2013, , .		3
194	Predictive linear regression model for microinverter internal temperature. , 2014, , .		3
195	Mirror augmented photovoltaics and time series analytics of the I–V curve parameters. , 2014, , .		3
196	A data science approach to understanding photovoltaic module degradation. , 2015, , .		3
197	EL and I-V Correlation for Degradation of PERC vs. Al-BSF Commercial Modules in Accelerated Exposures. , 2018, , .		3
198	Performance Loss Rates of PV systems of Task 13 database. , 2019, , .		3

#	Article	IF	CITATIONS
199	Inâ€situ observation of AlN formation from Niâ€Al solution using an electromagnetic levitation technique. Journal of the American Ceramic Society, 2020, 103, 2389-2398.	3.8	3
200	Toward Findable, Accessible, Interoperable and Reusable (FAIR) Photovoltaic System Time Series Data. , 2021, , .		3
201	Degradation mechanisms and partial shading of glass-backsheet and double-glass photovoltaic modules in three climate zones determined by remote monitoring of time-series current–voltage and power datastreams. Solar Energy, 2021, 224, 1291-1301.	6.1	3
202	Degradation analysis of field-exposed photovoltaic modules with non-fluoropolymer-based backsheets. , 2017, , .		3
203	Electronic and Vibrational Excitations in Polysilanes and Oligomers. Molecular Crystals and Liquid Crystals, 1992, 216, 13-19.	0.3	2
204	Metrology of etched quartz and chrome embedded phase shift gratings using scatterometry. , 1995, , .		2
205	Non-tracked mirror-augmented photovoltaic design and performance. , 2012, , .		2
206	Thermal performance of microinverters on dual-axis trackers. Proceedings of SPIE, 2014, , .	0.8	2
207	Continuity of States in Cholesteric - Line Hexatic Transition in Univalent and Polyvalent Salt DNA Solutions. Materials Research Society Symposia Proceedings, 2014, 1619, 1.	0.1	2
208	Detecting heterogeneity in PV modules from massive real-world "step―I-V curves: A machine learning approach. , 2016, , .		2
209	Photon Management through Virusâ€Programmed Supramolecular Arrays. Advanced Biology, 2017, 1, 1700088.	3.0	2
210	Photovoltaic Array Differential Backside Exposure Conditions: Backsheet Degradation and Site Design. , 2017, , .		2
211	Degradation Models of Photovoltaic Module Backsheets Exposed to Diverse Real World Condition. , 2017, , .		2
212	Wavelength Sensitivity in Photodegradation of Polymer PV Backsheets. , 2018, , .		2
213	Degradation of PERC and Al-BSF Photovoltaic Cells with Differentiated Mini-module Packaging Under Damp Heat Exposure. , 2019, , .		2
214	Nanomechanical and Fluorescence Characterizations of Weathered PV Module Encapsulation. IEEE Journal of Photovoltaics, 2021, 11, 725-730.	2.5	2
215	Degradation of photovoltaic backsheet materials under multi-factor accelerated UV light exposures. , 2017, , .		2
216	Characterization of Real-world and Accelerated Exposed PV Module Backsheet Degradation. , 2019, , .		2

#	Article	IF	CITATIONS
217	Automatic Spectral Database and Archive System for Optical Spectroscopy. Applied Spectroscopy, 1990, 44, 1221-1226.	2.2	1
218	Relation between Local Composition, Chemical Environment and Phase Shift Behavior in Cr-Based Oxycarbonitride Thin Films. Materials Research Society Symposia Proceedings, 2000, 636, 531.	0.1	1
219	Performance of a Low-Cost, Low-Concentration Photovoltaic Module. , 2011, , .		1
220	Solar radiation durability of materials, components and systems for photovoltaics. , 2011, , .		1
221	GaN microdomes for broadband omnidirectional antireflection for concentrator photovoltaics. , 2013, , .		1
222	Interfacial modifiers for enhanced stability and reduced degradation of Cu(In,) Tj ETQq0 0 0 rgBT /Overlock 10 Tf	50 542 T	d (Ça)Se <ir< td=""></ir<>
223	Characterizing the weathering induced haze formation and gloss loss of poly(ethylene-terephthalate) via MaPd:RTS spectroscopy. , 2016, , .		1
224	Cross-correlation Analysis of the Indoor Accelerated and Real World Exposed Photovoltaic Systems Across Multiple Climate Zones. , 2018, , .		1
225	Performance Evaluation of Commercially Relevant p-Type Silicon Cell Architectures. , 2019, , .		1
226	Learnings from developing an applied data science curricula for undergraduate and graduate students. MRS Advances, 2020, 5, 347-353.	0.9	1
227	Degradation of Monofacial Double Glass and Glass Backsheet Photovoltaic Modules with Multiple Packaging Combinations. , 2021, , .		1

228	Evaluation of cooling setpoint setback savings in commercial buildings using electricity and exterior temperature time series data. Energy, 2021, 233, 121117.	8.8	1	
229	Simulations and Experiments of Tunable GaN Microdomes for Broadband Omnidirectional Antireflection. , 2013, , .		1	
230	Degradation analysis of polyamide-based backsheets in field photovoltaic modules under different climatic conditions (Conference Presentation). , 2018, , .		1	
231	Symposium for Electronic Structure of Ceramics. Journal of the American Ceramic Society, 1990, 73, 3133-3133.	3.8	0	
232	TiSi-nitride attenuating phase-shift photomask for 193-nm lithography. , 1998, 3546, 514.		0	
000	Insights into the Electronic Structure of Ceramics Through Quantitative Analysis of Valence	0.4	0	

 ²³³ Electron Energy-Loss Spectroscopy (VEELS). Microscopy and Microanalysis, 1999, 5, 666-667.
 0.4
 0

 Object dependent properties of mirrors for PV applications studied under accelerated weathering
 0

Object dependent properties of mirrors for PV applications studied under accelerated weathering protocols. , 2013, , .

#	Article	IF	CITATIONS
235	Dependence of the strength of van der Waals interactions on the details of the dielectric response variation. Materials Research Society Symposia Proceedings, 2014, 1648, 1.	0.1	Ο
236	Optical Properties and van der Waals-London Dispersion Interactions in Inorganic and Biomolecular Assemblies. Materials Research Society Symposia Proceedings, 2014, 1619, 1.	0.1	0
237	Quantify Photovoltaic Module Degradation using the Loss Factor Model Parameters. , 2017, , .		0
238	Initial Stability of PERC vs. Al-BSF Cells. , 2018, , .		0
239	Future Trend and Perspectives. , 2019, , 329-336.		Ο
240	Open Circuit Voltages for PERC Local Back Surface Fields Directly Resolved at the Nanoscale. , 2019, , .		0
241	Properties of PV Cell Fractures and Effects on Performance of Al-BSF and PERC Modules. , 2021, , .		Ο
242	Novel Process Methodology for Uniformly Cutting Nanotubes. Materials Research Society Symposia Proceedings, 2003, 772, 151.	0.1	0
243	Optical Studies of Polysilanes. , 1991, , 143-148.		Ο
244	Quantitative analysis of spatially resolved valence electron energy-loss spectra for electronic structure studies of grain boundaries and thin intergranular films. Proceedings Annual Meeting Electron Microscopy Society of America, 1995, 53, 314-315.	0.0	0
245	Immersion Lithography. , 2016, , 1510-1516.		Ο
246	Immersion Lithography Materials. , 2016, , 1517-1523.		0
247	Cross-correlation of backsheet degradation between real-world exposed modules and accelerated exposures of backsheet materials (Conference Presentation). , 2016, , .		Ο
248	Model development of degradation of PV modules backsheet with locating place of module. , 2017, , .		0
249	Characterizing the weathering induced changes in optical performance and properties of poly(ethylene-terephthalate) via MaPd:RTS spectroscopy. , 2017, , .		Ο
250	Automated pipeline framework for processing of large-scale building energy time series data. , 2020, 15, e0240461.		0
251	Automated pipeline framework for processing of large-scale building energy time series data. , 2020, 15, e0240461.		0
252	Automated pipeline framework for processing of large-scale building energy time series data. , 2020, 15,		0

252 e0240461.

#	Article	IF	CITATIONS
253	Automated pipeline framework for processing of large-scale building energy time series data. , 2020, 15, e0240461.		0